JOURNAL OF MATERIALS SCIENCE 20 (1985) 3993–4000

Surface, grain-boundary and interfacial energies in Al_2O_3 and Al_2O_3–Sn, Al_2O_3–Co systems

P. NIKOLOPOULOS
Department of Chemical Engineering, University of Patras, Patras, Greece

Using the multiphase equilibrium method for the measurement of contact angles, the surface and grain-boundary energies of polycrystalline Al_2O_3 in the temperature range of 1473 to 1923 K were determined. Linear temperature functions were obtained by extrapolation for both quantities between absolute zero and the melting point of Al_2O_3. The temperature dependence of the surface and grain boundary energies can be expressed as

$$\gamma_{Al_2O_3} = 2.559 - 0.784 \times 10^{-3} T \ (J\ m^{-2})$$

and

$$\gamma_{Al_2O_3\text{–}Al_2O_3} = 1.913 - 0.611 \times 10^{-3} T \ (J\ m^{-2})$$

respectively. The interfacial energies of Al_2O_3 in contact with the molten metals tin and cobalt revealed a linear dependence on temperature.

1. Introduction

Surface energy plays an important role in the powder technological consolidation of single as well as multiphase materials. The driving force for the sinterability of materials is the reduction of the free surface area, and thus a decrease in the total energy of the system. In the presence of a liquid phase during sintering of composites, e.g. ceramics and metals, the density, microstructure and mechanical properties are influenced by the wetting behaviour at the interface.

The wetting in a solid–liquid system in thermodynamic equilibrium is characterized by the wetting angle. Its magnitude depends on the temperature and the surface as well as on the interfacial energies of the phases in contact.

This paper describes experiments that have been carried out to determine the temperature functions of the surface and grain-boundary energies of polycrystalline alumina. In addition the interfacial energies in the Al_2O_3–Sn and Al_2O_3–Co systems are given.

2. Multiphase equilibrium method

In order to determine the surface and grain boundary energies, four sets of experiments are necessary to measure the equilibrium angles that develop at the interface [1, 2]:

(a) Measurement of the groove angle (ψ) in a nonadsorbing gas atmosphere by means of thermal etching (Fig. 1a). The following equation is then valid,

$$\gamma_{ss} = 2\,\gamma_{sv} \cos\frac{\psi}{2} \quad (1)$$

(b) Measurement of the groove angle (ψ^*) in an atmosphere contaminated with metal vapour (Fig. 1b). The following equation is then valid,

$$\gamma_{ss} = 2\,\gamma^*_{sv} \cos\frac{\psi^*}{2} \quad (2)$$

(c) Measurement of the dihedral angle (ϕ) in the presence of a liquid phase (Fig. 1c). The following equation is then valid,

0022–2461/85 $03.00 + .12

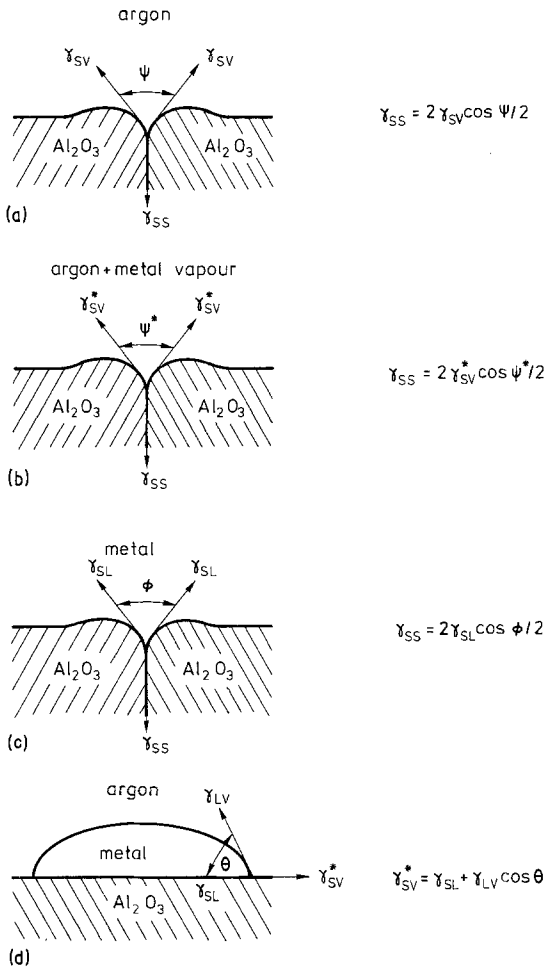

Figure 1 Schematic diagram in a solid–liquid–gas system in equilibrium showing groove, dihedral and wetting angles.

$$\gamma_{SS} = 2\,\gamma_{SL}\cos\frac{\phi}{2} \qquad (3)$$

(d) Measurement of the wetting angle (θ) with the aid of the sessile drop experiment (Fig. 1d). The following equation is then valid,

$$\gamma^*_{SV} = \gamma_{SL} + \gamma_{LV}\cos\theta \qquad (4)$$

The symbols in the above equations mean:

ψ, ψ^* = groove angles
ϕ = dihedral angle
θ = wetting angle
$\gamma_{SV}, \gamma^*_{SV}$ = surface energies
γ_{SS} = grain boundary energy
γ_{SL} = interfacial energy

Indices: L = liquid, V = vapour, S = solid.

Combining Equations 1 to 4 we obtain

$$\gamma_{SV} = \gamma_{LV}\cos\theta\,\frac{\cos\frac{\phi}{2}\cos\frac{\psi^*}{2}}{\cos\frac{\psi}{2}\left(\cos\frac{\phi}{2} - \cos\frac{\psi^*}{2}\right)} \qquad (5)$$

To determine the surface energy γ_{SV}, the only additional datum required is the surface energy of the liquid metal, which is available in the literature.

3. Experimental procedure

Polycrystalline alumina Al23 (tradename of Friedrichsfeld Co, West Germany) with a purity of > 99.5 wt % was used in the wetting experiments. The purity of the metals tin and cobalt was 99.9999 wt % and 99.998 wt % respectively. The as-received Al_2O_3 had a density 3.7 to 3.95 $Mg\,m^{-3}$ and a grain size of 10 to 20 μm. Discs of 20 mm diameter and 3 mm thickness were used in the experiments.

The wetting angle was measured with an apparatus specially constructed for our purpose [3]. The samples were heated with an induction coil. The measurements were carried out in a purified argon atmosphere (99.999%). The viewing parts were used to photograph the sessile drops as well as to measure the temperature by optical pyrometry. The precision of the temperature measurements is ± 20 K.

Optical interferometry was used to measure the groove angles (ψ, ψ^*) and the dihedral angle (ϕ). In order to observe the undisturbed interference patterns, large grains are desirable. For this reason, Al_2O_3 (Al25) with a purity of > 99.5 wt % was used. Its density was 2.8 $Mg\,m^{-3}$, the grain size being 50 to 150 μm.

Metallographically polished samples were thermally etched in one of the following:

(a) A dry argon atmosphere (groove angle ψ).

(b) Argon with a metal-contaminated atmosphere (groove angle ψ^*). A crucible with tin or cobalt metal was introduced in the vicinity of the sample in order to provide the desired metal vapour contamination.

(c) For the measurement of the dihedral angle (ϕ), the metal was melted in an argon atmosphere whilst in contact with Al_2O_3. Due to the insufficient wetting, the metal was then removed from the Al_2O_3 surface before carrying out the measurements.

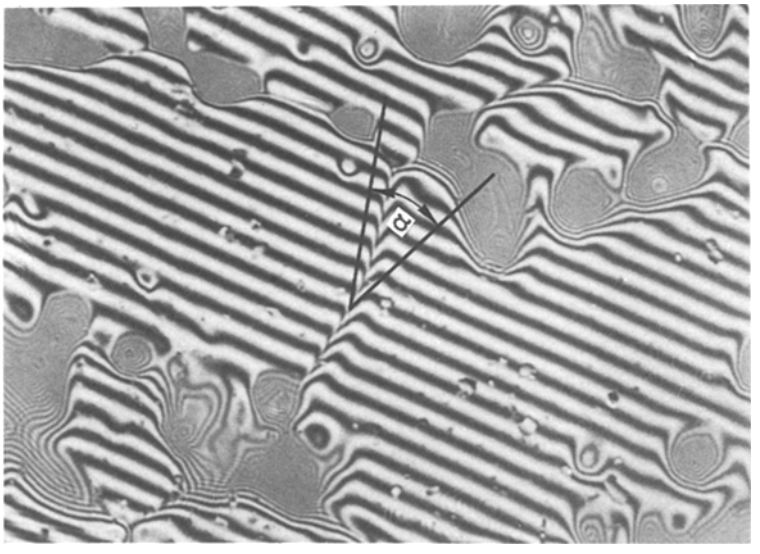

Figure 2 Interference patterns to obtain the groove angle ψ of Al_2O_3 in argon ($T = 1783\,K$, $t = 16\,h$, $\lambda = 589\,nm$, $m = 1360\times$)

The true root angles (ψ, ψ^*, ϕ) can be calculated from the apparent root angle α with the aid of the following equation [4]:

$$\tan\frac{\psi}{2} = \frac{2d}{1.11\lambda m}\tan\frac{\alpha}{2} \qquad (6)$$

where d = width between the groove shoulders, λ = wavelength of the light source and m = magnification. The factor 1.11 is used to correct the effect of the large aperture of the objective lens. Fig. 2 shows the interference patterns thus obtained. Since it is not possible to discriminate between grain boundaries that are not perpendicular to the plane sections, only those angles were considered in which the interference patterns continued in the same way approximately on both sides of the grooves, showing no drastic shift (Fig. 2).

4. Experimental results

4.1. Wetting angle (θ)

Owing to the fact that measured wetting angle (θ) in the Al_2O_3–Sn and Al_2O_3–Co systems was greater than 90°, a computer program was written based on the tables of Bashfort and Adams [5] to calculate θ. The linear temperature functions of the surface energy of the liquid metals tin [6] and cobalt [7, 8] are given in the literature as

$$\gamma_{LV}(Sn) = 0.544 - 0.07\times10^{-3}(T - T_m)\ \ J\,m^{-2} \qquad (7)$$

and

$$\gamma_{LV}(Co) = 1.610 - 0.29\times10^{-3}(T - T_m)\ \ J\,m^{-2} \qquad (8)$$

TABLE I Wetting angles (θ), surface energies (γ_{LV}) and work of adhesion (W_a) in the Al_2O_3–Sn and Al_2O_3–Co systems

System	T (K)	θ (deg)	Median standard error	γ_{LV} ($J\,m^{-2}$)	$\gamma_{LV}\cos\theta$ ($J\,m^{-2}$)	W_a ($J\,m^{-2}$)
Al_2O_3–Sn	611	165.24	±1.82	0.537	−0.519	0.018
	726	161.74	±1.20	0.529	−0.502	0.027
	772	157.74	±3.52	0.525	−0.486	0.039
	975	148.26	±2.52	0.511	−0.435	0.076
	1183	141.96	±1.21	0.497	−0.391	0.106
	1280	138.95	±1.89	0.490	−0.370	0.120
Al_2O_3–Co	1888	128.20	±1.41	1.575	−0.974	0.601
	1973	123.91	±1.50	1.551	−0.865	0.686
	2023	120.10	±1.30	1.536	−0.770	0.766
	2113	116.68	±1.00	1.510	−0.678	0.832

for $T \geqslant T_m$ = melting point; $T_m(Sn) = 505\,K$, $T_m(Co) = 1768\,K$.

The results obtained from the sessile drop experiments are summarized in Table I, which also includes the work of adhesion calculated with aid of the equation

$$W_a = \gamma_{LV}(1 + \cos\theta) \quad (9)$$

It can be seen from Table I that the work of adhesion as well as the product $\gamma_{LV}\cos\theta$ are, as expected, linear functions of temperature.

In the case of the Al_2O_3–Sn system we obtain

$$\gamma_{LV}\cos\theta = -0.547 + 0.230 \times 10^{-3}(T - T_m)\ J\,m^{-2} \quad (R = 0.9983) \quad (10)$$

and

$$W_a = 0.160 \times 10^{-3}(T - T_m)\ J\,m^{-2} \quad (R = 0.9967) \quad (11)$$

In the case of the Al_2O_3–Co system we obtain

$$\gamma_{LV}\cos\theta = -1.132 + 1.342 \times 10^{-3}(T - T_m)\ J\,m^{-2} \quad (R = 0.9943) \quad (12)$$

and

$$W_a = 0.478 + 1.053 \times 10^{-3}(T - T_m)\ J\,m^{-2} \quad (R = 0.9967) \quad (13)$$

with R = coefficient of correlation.

4.2. Groove angles (ψ, ψ^*) and dihedral angle (ϕ)

Table II shows the measured groove angles (ψ, ψ^*) and dihedral angle (ϕ). The annealing times chosen were 5 to 20 h at 1473 K, 3 to 20 h at 1623 K, 2 to 16 h at 1783 K and 1 to 5 h at 1923 K in argon (100 kPa). The results reveal that in the temperature range chosen the groove angle ψ is practically independent of annealing temperature and time. The ratio γ_{SS}/γ_{SV} (Equation 1) remains practically constant. However, the angle ϕ is a function of temperature, and for a given combination with a metal it decreases with increasing temperature.

5. Surface and grain-boundary energies

From the experimental results shown in Table II and the values of the expression $\gamma_{LV}\cos\theta$ (Equations 10 and 12) the surface energy (γ_{SV}) of Al_2O_3 can be calculated using Equation 5. The grain-boundary energy can then be determined using Equation 1. The results obtained are shown in Table III.

The ratio of the surface to the grain-boundary energy (γ_{SS}/γ_{SV}) in Al_2O_3 varies between 0.70 and 0.74. This value agrees reasonably well with values obtained with UO_2 in the same temperature range and atmosphere (0.54 to 0.67 [1] and 0.54 to 0.58 [2]). Kingery [9] reports a value of 0.49 under different conditions, namely 2123 K and a helium atmosphere. McLean and Hondros [10] report a much lower value ($\gamma_{SS}/\gamma_{SV} = 0.08$) measured in air at 1673 K.

Fig. 3 shows the calculated values of the surface energy of Al_2O_3 as a function of temperature. In the temperature range covered only one value is available in the literature [10], and this is also shown in Fig. 3. If the surface energy is assumed to be a linear function of temperature we can write

$$\frac{d\gamma_{SV}}{dT} = -0.784 \times 10^{-3}\ J\,m^{-2}\,K^{-1} \quad 1473 \leqslant T \leqslant 1923\ K \quad (14)$$

Extrapolation to higher temperatures gives a value of $0.894\,J\,m^{-2}$ at 2123 K, which shows good agreement with the value of $0.905\,J\,m^{-2}$ reported by Kingery [9]. Extrapolation to the melting point of Al_2O_3 ($T = 2323\,K$) gives a value of $0.728\,J\,m^{-2}$. Based on the theoretical considerations of Skapski [11], Allen [6] concluded that for metals at the melting point $\gamma_{SV} = 1.1\gamma_{LV}$. Assuming that this relation is also valid for oxides at the melting point, we can deduce a value of $\gamma_{LV} = 0.671\,J\,m^{-2}$ for Al_2O_3 at its melting point. This value shows good agreement with the surface energies of molten Al_2O_3 reported by Kingery [12] ($0.690\,J\,m^{-2}$); Rasmussen and Nelson [13] (0.638 and $0.574\,J\,m^{-2}$ using two separate methods), and Bartlett and Hall [14] ($0.551\,J\,m^{-2}$ at 2423 K).

Extrapolation to room temperature gives a value of $2.325\,J\,m^{-2}$. Fricke [15] determined a value of $0.560\,J\,m^{-2}$ from the heat of solution of crystals and Bruce [16] obtained a value of $1.2\,J\,m^{-2}$ from thermodynamic data. Both values are much lower than those obtained in the present work. Often the value of Kingery [9] has

TABLE II Groove angles (ψ, ψ^*) and dihedral angle (ϕ), with median standard errors

T (K)	System	ψ (deg)	Angles†	System	ψ^* (deg)	Angles†	System	ϕ (deg)	Angles†
1473	Al_2O_3 + Ar	138.26 ± 0.98	18	Al_2O_3 + Sn (vapour) + Ar	139.18 ± 0.77	38	Al_2O_3 + Sn (metal)	146.92 ± 0.72	39
1623	Al_2O_3 + Ar	136.66 ± 0.51	83	Al_2O_3 + Sn (vapour) + Ar	137.56 ± 0.88	33	Al_2O_3 + Sn (metal)	145.53 ± 0.45	78
1783	Al_2O_3 + Ar	139.30 ± 0.29	150	Al_2O_3 + Co (vapour) + Ar	138.90 ± 0.41	117	Al_2O_3 + Co (metal)	159.55 ± 0.24	159
1923	Al_2O_3 + Ar	138.74 ± 0.54	91	Al_2O_3 + Co (vapour) + Ar	137.11 ± 0.61	75	Al_2O_3 + Co (metal)	157.86 ± 0.47	55

†Number of measured groove and dihedral angles

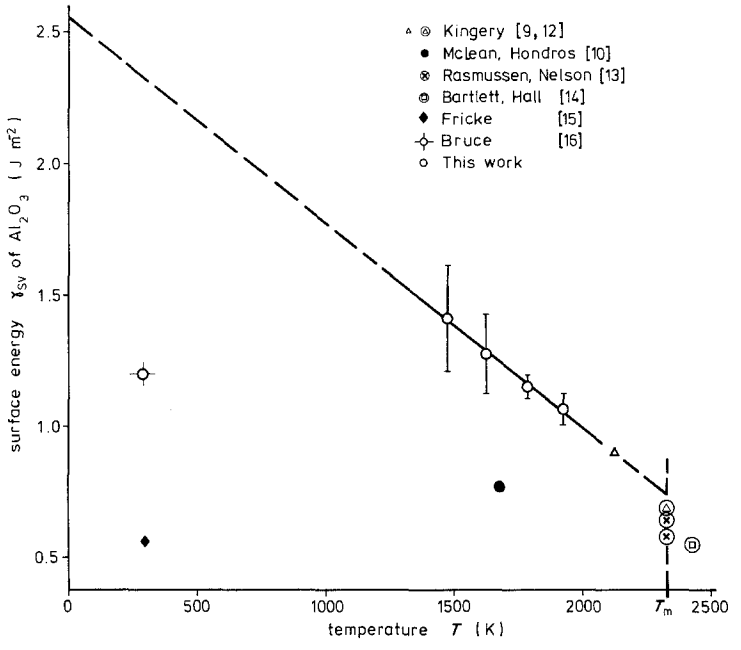

Figure 3 The temperature dependence of the surface energy of Al_2O_3.

been used at varying temperatures with the temperature coefficient $d\gamma_{SV}/dT = -0.1 \times 10^{-3}$ J m^{-2} K^{-1} for extrapolation. This coefficient has generally been used not only for Al_2O_3 but several oxides [17].

Microfracture experiments have also been used to determine the fracture surface energy of polycrystalline alumina at room temperature [18–20]. The data for a material of comparable porosity and grain size is of an order of magnitude higher (20 to 30 J m^{-2}).

For the entire temperature range between absolute zero and the melting point for Al_2O_3 (Fig. 3), the linear temperature function can be expressed as:

$$\gamma_{SV}(Al_2O_3) = 2.559 - 0.784 \times 10^{-3} T \text{ J m}^{-2} \quad (R = 0.9978) \quad (15)$$

The grain boundary energy of Al_2O_3 can be expressed as

$$\gamma_{SS}(Al_2O_3\text{–}Al_2O_3) = 1.913 - 0.611 \times 10^{-3} T \text{ J m}^{-2} \quad (R = 0.9837) \quad (16)$$

TABLE III Surface (γ_{SV}) and grain-boundary energies (γ_{SS}) of Al_2O_3

T (K)	γ_{SV} (J m^{-2})	γ_{SS} (J m^{-2})	γ_{SS}/γ_{SV}
1473	1.410 ± 0.203	1.004 ± 0.146	0.712
1623	1.283 ± 0.151	0.947 ± 0.112	0.738
1783	1.148 ± 0.040	0.799 ± 0.028	0.696
1923	1.061 ± 0.061	0.747 ± 0.044	0.704

6. Interfacial energies

With the experimental values of the groove angle ψ^* and dihedral angle ϕ (Table II) and the calculated values of the grain boundary energy γ_{SS} of Al_2O_3 (Table III), γ^*_{SV} and γ_{SL} in the systems Al_2O_3–Sn and Al_2O_3–Co can be obtained using Equations 2 and 3 (Table IV). It can be seen that γ_{SV} and γ^*_{SV} do not vary significantly, considering the accuracy of the data. It seems, therefore, that the metal vapour does not have a major influence on the surface energy of Al_2O_3. Under these conditions we can use γ_{SV} instead of γ^*_{SV} in Equation 4 and obtain

$$\gamma_{SL} = \gamma_{SV} - \gamma_{LV} \cos\theta \quad (17)$$

Using the linear temperature functions of $\gamma_{LV} \cos\theta$ (Equations 10 and 12) and γ_{SV} (Equation 15) in Equation 17, we obtain the temperature functions of the interfacial energies in the Al_2O_3–Sn and Al_2O_3–Co systems:

$$\gamma_{SL}(Al_2O_3\text{–Sn}) = 2.710 - 1.014 \times 10^{-3} (T - T_m) \text{ J m}^{-2} \quad (18)$$

TABLE IV Surface energy (γ^*_{SV}) of Al_2O_3 in the presence of metal vapour (argon atmosphere) and interfacial energy (γ_{SL}) of Al_2O_3–liquid metal

System	T (K)	γ^*_{SV} (J m^{-2})	γ_{SL} (J m^{-2})
Al_2O_3–Sn	1473	1.440 ± 0.210	1.764 ± 0.257
Al_2O_3–Sn	1623	1.309 ± 0.155	1.599 ± 0.189
Al_2O_3–Co	1783	1.138 ± 0.040	2.250 ± 0.079
Al_2O_3–Co	1923	1.022 ± 0.060	1.946 ± 0.115

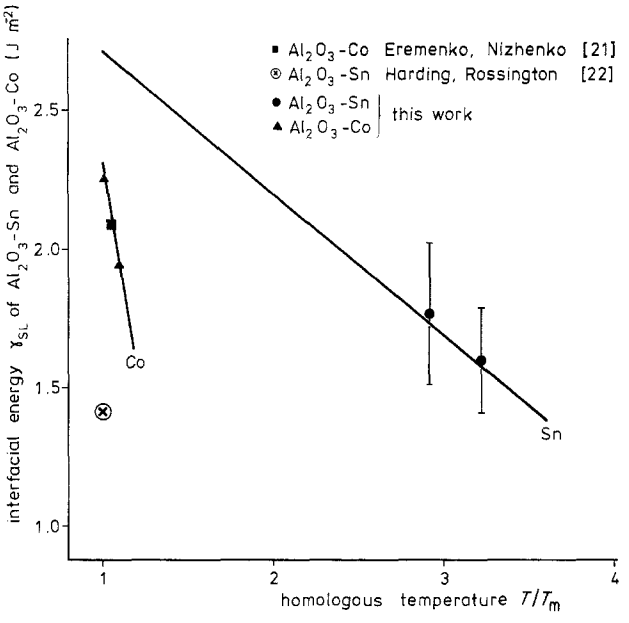

Figure 4 The temperature dependence of interfacial energy in the Al_2O_3–Sn and Al_2O_3–Co systems.

and

$$\gamma_{SL}\,(Al_2O_3\text{–Co}) = 2.305 - 2.126 \times 10^{-3}\,(T - T_m)\ \text{J m}^{-2} \qquad (19)$$

Fig. 4 shows the experimental results and the calculated linear temperature functions of the interfacial energy as a function of the homologous temperature (T/T_m). The agreement between the experimentally determined values of the interfacial energies (Table IV) and those calculated using Equation 17 is very good.

The values of the interfacial energies reported in the literature were obtained with the aid of Equation 17 using extrapolated values of the surface energy of Al_2O_3 determined by Kingery [9]. The value of the interfacial energy in the Al_2O_3–Co system reported by Eremenko and Nizhenko [21] at 1873 K in a vacuum (2.095 J m^{-2}) is in good agreement with our determination using Equation 19 (2.082 J m^{-2}). On the other hand, for the low-melting metal tin in the Al_2O_3–Sn system the value reported by Harding and Rossington [22] (1.404 J m^{-2}) is lower by almost a factor of two compared to ours (2.710 J m^{-2}). A correction using Equations 15 and 17 for $\theta = 123°$ and $\gamma_{LV}(Sn) = 0.513$ J m^{-2} [22] gives a much higher value of the interfacial energy (γ_{SL} = 2.475 J m^{-2}).

Throughout this study the various interfacial energies are assumed to be isotropic, since the surface energy of polycrystalline Al_2O_3 in the temperature range investigated (1473 to 1923 K) can be considered as independent of the crystallographic orientation [23, 24].

7. Conclusions

1. The wetting angle θ in the Al_2O_3–Sn and Al_2O_3–Co systems was determined experimentally. It was found that these metals show a poor wetting behaviour at their melting point ($\theta > 90°$).

2. The surface and grain-boundary energies of Al_2O_3 in the temperature range 1473 to 1923 K were calculated from measurements of the groove, dihedral and wetting angles between the phases in equilibrium. The linear temperature coefficient of the surface energy of Al_2O_3 was determined as

$$\frac{d\gamma_{SV}}{dT} = -0.784 \times 10^{-3}\ \text{J m}^{-2}\ \text{K}^{-1}$$

3. The temperature functions of the interfacial energies in the Al_2O_3–Sn and Al_2O_3–Co systems were obtained assuming that the influence of metal vapour on the surface energy of Al_2O_3 can be neglected.

Acknowledgements

Part of this work was performed during the author's stay at the Institut für Material- und Festkörperforschung of the Nuclear Research Center Karlsruhe. The author appreciates the

technical assistance of Mr F. Gehlen and Mr E. Parissis as well as fruitful discussions with Dr S. Nazaré.

References

1. E. N. HODKIN and M. G. NICHOLAS, *J. Nucl. Mater.* **47** (1973) 23.
2. P. NIKOLOPOULOS, S. NAZARÉ and F. THÜMMLER, *ibid.* **71** (1977) 89.
3. P. NIKOLOPOULOS and B. SCHULZ, *ibid.* **82** (1979) 172.
4. S. AMELINCKX, N. F. BINNENDIJK and E. DEKEYSER, *Physica* **19** (1953) 1173.
5. F. BASHFORT and S. C. ADAMS, "An Attempt to test the theories of capillary action" (University Press, Cambridge, 1883) p. 63.
6. B. C. ALLEN, "Liquid Metals", edited by S. Z. Beer (Dekker, New York, 1972) p. 161.
7. L. ZAGAR and W. BERNHARDT, "Forschungsberichte des Landes Nord-Rheinwestfahlen", Nr. 1733 (Westdeutscher Verlag, Köln, 1966) p. 65.
8. A. R. MIEDEMA and R. BOOM, *Z. Metallkde.* **69** (1978) 183.
9. W. D. KINGERY, *J. Amer. Ceram. Soc.* **37** (1954) 42.
10. M. McLEAN and E. D. HONDROS, *J. Mater. Sci.* **6** (1971) 19.
11. A. S. SKAPSKI, *Acta Metall.* **4** (1956) 576.
12. W. D. KINGERY, *J. Amer. Ceram. Soc.* **42** (1959) 6.
13. J. J. RASMUSSEN and R. P. NELSON, *ibid.* **54** (1971) 398.
14. R. W. BARTLETT and J. K. HALL, *Amer. Ceram. Soc. Bull.* **44** (1965) 444.
15. R. FRICKE, *Kolloid Z.* **96** (1941) 213.
16. R. H. BRUCE, "Science of Ceramics", edited by G. H. Stewart (Academic, London, 1965) p. 359.
17. D. T. LIVEY and P. MURRAY, in 2nd Plansee Seminar, edited by F. Benesovsky, 1955 (Springer, Wien, 1956) p. 375.
18. R. W. DAVIDGE and G. TAPPIN, *J. Mater. Sci.* **3** (1968) 165.
19. R. P. WAHI and B. ILSCHNER, *ibid.* **15** (1980) 875.
20. M. T. LAUGIER, *ibid.* **19** (1984) 254.
21. V. N. EREMENKO and V. I. NIZHENKO, *Russ. J. Phys. Chem.* **35** (1961) 638.
22. F. L. HARDING and D. R. ROSSINGTON, *J. Amer. Ceram. Soc.* **53** (1970) 87.
23. S. K. RHEE, *ibid.* **55** (1972) 300.
24. W. M. ROBERTSON and P. CHANG, "Materials Science Research", edited by W. W. Kriegel and H. Palmour, III (Plenum, New York, 1966) p. 49.

Received 10 August
and accepted 18 December 1984